4-2019

Regenerative Ionic Currents and Bistability

Gregory D. Conradi Smith
William & Mary, gdsmit@wm.edu

11 Regenerative Ionic Currents and Bistability

Membranes with regenerative ionic currents such as $I_{\mathrm{Ca_V}}$ and I_{Kir} may exhibit more than one steady state voltage. The phase diagram of the current balance equation gives insight into the phenomenon of membrane bistability in motoneurons and cerebellar Purkinje cells.

11.1 Regenerative Currents and Membrane Bistability

The dynamics of voltage in membranes that express nonlinear ionic currents can be more complex than what is observed in passive membrane models (Fig. 8.7). Consider a neuron whose membrane includes a passive leak (I_L) but also a voltage-gated Ca^{2+} current ($I_{\mathrm{Ca_V}}$) mediated by high-voltage activated L-type calcium channels. The current balance equation for the model is

$$C\frac{dV}{dt} = I_{app} - \underbrace{\bar{g}_{\mathrm{Ca_V}} m_\infty(V)(V - E_{\mathrm{Ca}})}_{I_{\mathrm{Ca_V}}(V)} - \underbrace{g_L(V - E_L)}_{I_L(V)} . \tag{11.1}$$

Steady states of the $I_{\mathrm{Ca_V}} + I_L$ membrane model are found by setting $dV/dt = 0$ in Eq. 11.1. A steady state voltage V_{ss} solves the nonlinear algebraic expression,

$$I_{app} = \underbrace{\bar{g}_{\mathrm{Ca_V}} m_\infty(V_{ss})(V_{ss} - E_{\mathrm{Ca}})}_{I_{\mathrm{Ca_V}}(V_{ss})} + \underbrace{g_L(V_{ss} - E_L)}_{I_L(V_{ss})} . \tag{11.2}$$

When the applied current is zero ($I_{app} = 0$), steady states of Eq. 11.1 are given by V_{ss} that solve $0 = I_{ion}(V_{ss})$ where $I_{ion} = I_{\mathrm{Ca_V}} + I_L$ is the total ionic membrane current. Because $m_\infty(V)$ is nonlinear, analytically solving Eq. 11.2 results in an unwieldy and unenlightening expression. However, an approach based on analytical geometry leads to considerable insight.

Fig. 11.1 plots current-voltage relations for $I_{\mathrm{Ca_V}}$, I_L and their sum I_{ion}. Interestingly, the total ionic current $I_{ion}(V)$ reverses *three times*. We will denote the three voltages for

https://doi.org/10.1017/9780511793905.015 Published online by Cambridge University Press

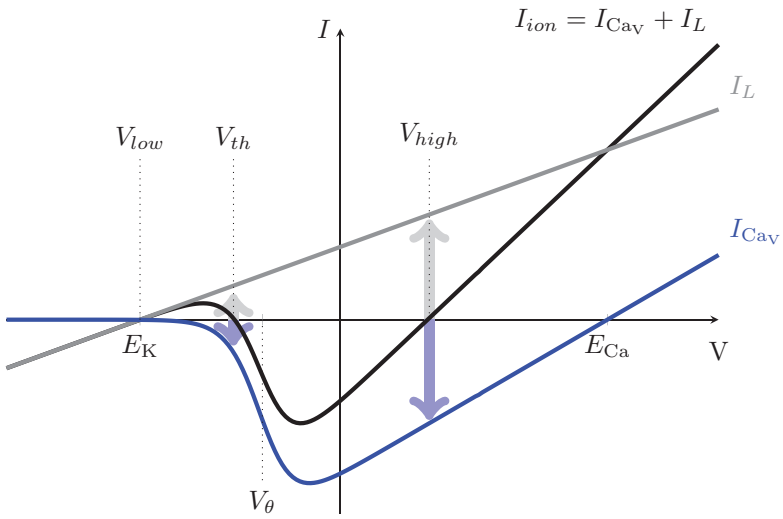

Figure 11.1 The sum of ionic currents $I_{ion} = I_{\mathrm{Ca_V}} + I_L$ may have three intersections with the horizontal axis. *Question*: What are the biological meanings of the parameters V_θ and V_{th}? How would you locate these voltages on the horizontal axis?

which $I_{ion} = 0$ as V_{low}, V_{th} and V_{high} (dotted lines). When $I_{app} = 0$ these steady state voltages and the reversal potentials E_{K} and E_{Ca} are related as follows,

$$E_L \approx V_{low} < V_{th} < 0 < V_{high} < E_{\mathrm{Ca}}\,.$$

The gray arrows in Fig. 11.1 emphasize that zero ionic membrane current, $I_{ion}(V_{ss}) = 0$, implies that $I_{\mathrm{Ca_V}}$ and I_L are equal in magnitude but opposite in sign, that is, $I_{\mathrm{Ca_V}}(V_{ss}) = -I_L(V_{ss})$ for any V_{ss} solving Eq. 11.2 when $I_{app} = 0$.

Fig. 11.2 shows the phase diagram for the $I_{\mathrm{Ca_V}} + I_L$ membrane model. Filled and open circles indicate the steady state voltages V_{low}, V_{th} and V_{high}. Decorating the phase line with arrows showing the sign of dV/dt reveals that V_{low} and V_{high} are stable steady states, while V_{th} is unstable. Indeed, the number and stability of steady states is easily determined from qualitative features of the phase diagram,

$$\begin{array}{ccc} f'(V_{low}) < 0 & f'(V_{th}) > 0 & f'(V_{high}) < 0 \\ \text{(stable)} & \text{(unstable)} & \text{(stable)}, \end{array}$$

where $f(V)$ is the right side of Eq. 11.1. The unstable steady state V_{th} is a **repellor** that separates the **basins of attraction** associated with the two stable steady states, both of which are **attractors** (recall Section 3.3).

Fig. 11.3 shows solutions of Eq. 11.1 with a range of initial membrane potentials (-150 to $100\,\mathrm{mV}$). The trajectories show that the basin of attraction of the stable steady state at V_{low} is the phase line interval $(-\infty, V_{th})$ while the basin of attraction of V_{high} is (V_{th}, ∞). Note that trajectories whose initial value is close (but not equal) to the unstable steady state V_{th} increase or decrease relatively slowly (at least initially). This is consistent with the phase diagram of Fig. 11.2 that indicates $|dV/dt|$ is small when $V \approx V_{th}$.

When the initial membrane voltage is near either one of the two *stable* steady states (V_{low} or V_{high}), there is a gradual decay of the deviation from steady state,

https://doi.org/10.1017/9780511793905.015 Published online by Cambridge University Press

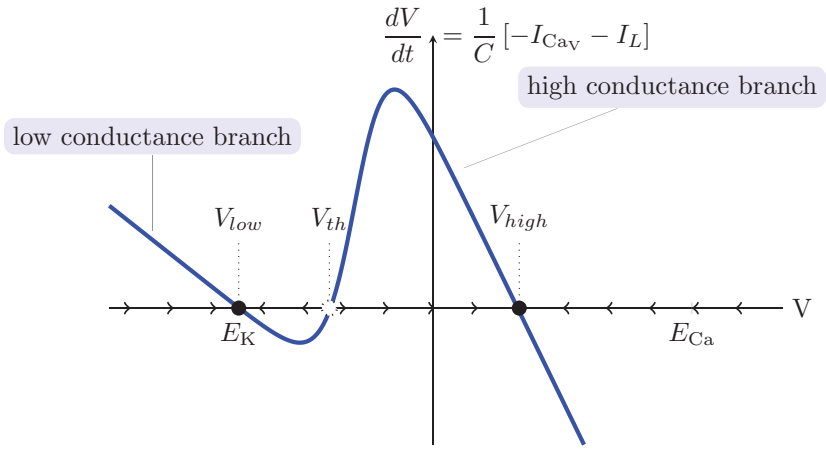

Figure 11.2 The phase diagram for a membrane that expresses $I_{\mathrm{Ca_V}}$ and I_L in the absence of applied current ($I_{app} = 0$). *Question*: When $V \approx V_{low}$ (or V_{high}), the dynamics are well approximated by exponential relaxation. For which steady state is the exponential time constant larger (slower relaxation)?

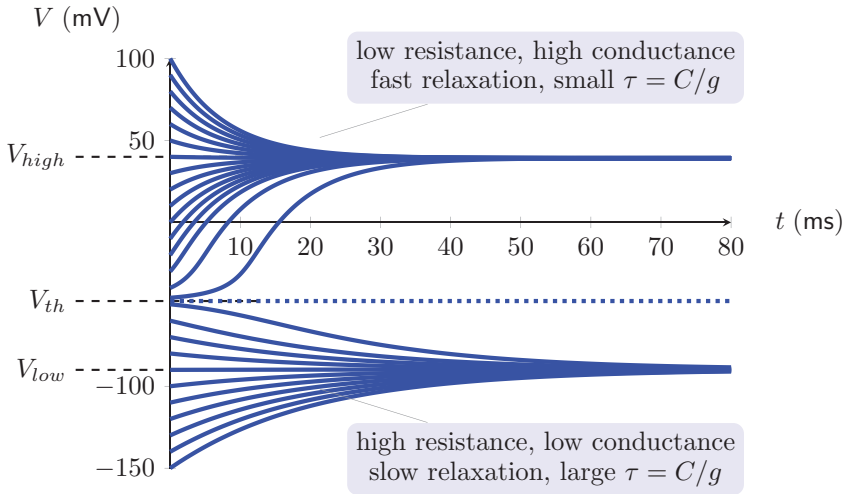

Figure 11.3 Solutions of the $I_{\mathrm{Ca_V}} + I_L$ membrane model reveal two stable steady state membrane potentials (bistability). Relaxation of voltage is faster near the depolarized steady state (V_{high}) than near the hyperpolarized steady state (V_{low}), consistent with Fig. 11.2.

$\Delta V = V - V_{ss}$. These trajectories cannot be bona fide exponential relaxations because Eq. 11.1 is nonlinear. However, it can be shown that the relaxation of V to either stable steady state is, at least ultimately, approximately exponential (see Discussion). Furthermore, the approximate exponential time constant associated to V_{high} is smaller (faster) than the time constant associated to V_{low}. Using the passive membrane time constant formula $\tau = C/g$, we see that the conductance of the cell membrane is greater when $V \approx V_{high}$ than when $V \approx V_{low}$. Indeed, the current-voltage relation for total ionic current (Fig. 11.3) confirms this: the slope $dI_{ion}/dV \ominus$ conductance is greater at V_{high} than at V_{low}.

https://doi.org/10.1017/9780511793905.015 Published online by Cambridge University Press

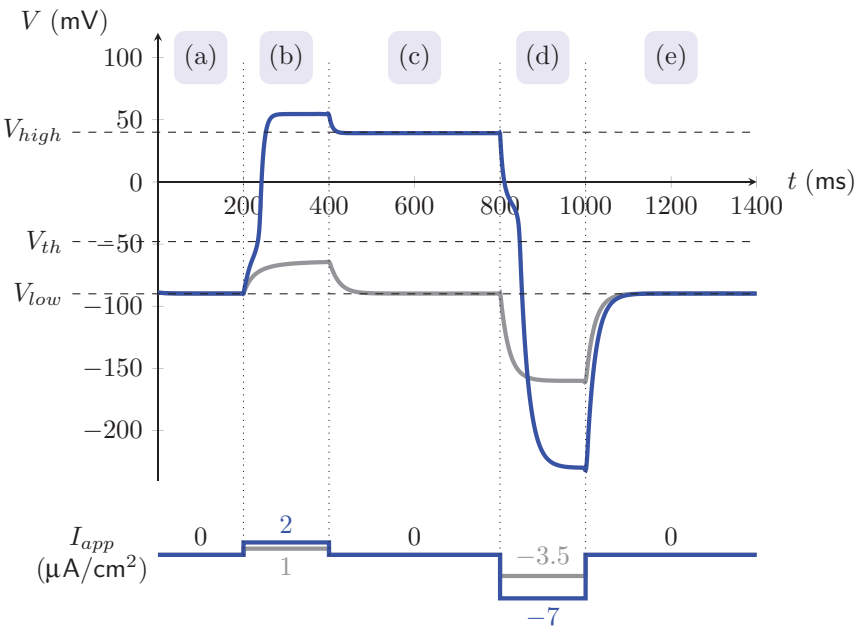

Figure 11.4 Bistability of the $I_{\mathrm{Cav}} + I_L$ membrane model (Eq. 11.1) observed in response to pulses of applied current (I_{app}).

11.2 Response of a Bistable Membrane to Applied Current Pulses

Fig. 11.4 shows numerically integrated solutions of the $I_{\mathrm{Cav}} + I_L$ membrane model (Eq. 11.1) when the applied current is a pulsatile function of time. $I_{app}(t)$ is zero for most of the simulation, but is depolarizing for 100 ms beginning at $t = 200$ ms, and hyperpolarizing for 100 ms beginning at $t = 800$ ms. The blue curve is the response when the first current pulse is depolarizing to such an extent ($I_{app} = 2\,\mu\mathrm{A/cm^2}$) that the membrane potential transitions from V_{low} to V_{high}. The voltage remains at V_{high} until the hyperpolarizing current pulse ($I_{app} = -7\,\mu\mathrm{A/cm^2}$) causes the membrane potential to return to V_{low}. Notice that the steady state voltage of the bistable membrane depends on the recent history of applied currents. This dynamical phenomenon is referred to as **hysteresis**. It is as though the bistable membrane is able to remember whether the most recent pulse of applied current was depolarizing or hyperpolarizing.

11.3 Membrane Currents and Fold Bifurcations

The gray curves in Fig. 11.4 repeat the sequence of depolarizing and hyperpolarizing pulses, but at half the magnitude. In this case, the depolarizing pulse is not sufficient to bring the membrane above the threshold V_{th}, so the membrane potential returns to V_{low} at the end of the first pulse. By repeating this calculation with lesser values of I_{app},

https://doi.org/10.1017/9780511793905.015 Published online by Cambridge University Press

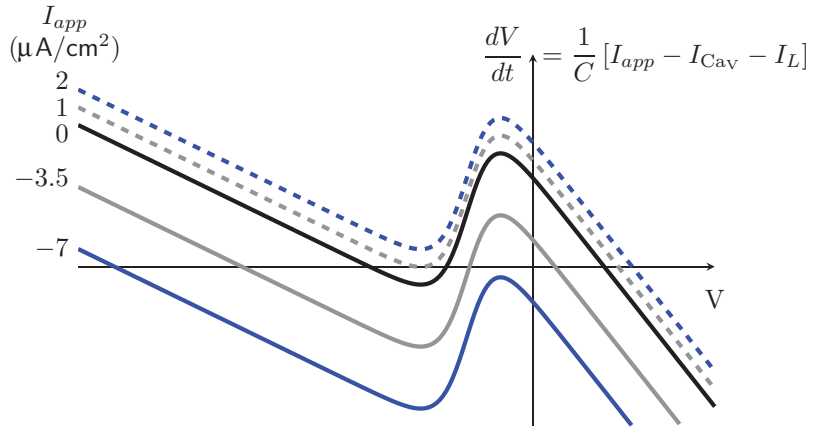

Figure 11.5 Phase diagram for a membrane model that includes $I_{\mathrm{Ca_V}}$ and I_L (Eq. 11.1). Shown are the five values of I_{app} used in Fig. 11.4.

one may determine the minimum amount of applied current required for the membrane voltage to surpass the threshold voltage (V_{th}) and enter the basin of attraction of V_{high}. In general, the current required will depend on the pulse duration.

Fig. 11.5 shows the phase diagram of the $I_{\mathrm{Ca_V}} + I_L$ membrane model for five values of I_{app}. For $I_{app} = 0$, the black curve indicates three steady states: two stable, one unstable (as in Fig. 11.2). When the applied current is sufficiently negative ($I_{app} = -7\,\mu\mathrm{A/cm^2}$), there is one hyperpolarized stable steady state (blue curve). When the applied current is sufficiently positive ($I_{app} = 2\,\mu\mathrm{A/cm^2}$), there is one depolarized stable steady state (blue dashed curve). The critical values of applied current lead to coalescence of a stable and unstable steady state. For example, the gray broken curve of Fig. 11.5 is nearly critical ($V_{low} \approx V_{th}$).

For current pulses of sufficiently long duration, Fig. 11.5 may be used to explain the dynamics of bistability in the $I_{\mathrm{Ca_V}} + I_L$ membrane model. For example, the step in applied current that occurs in epoch (b) of Fig. 11.4 depolarizes the membrane from $V \approx V_{low}$ into the basin of attraction associated with V_{high} when $I_{app} = 2\,\mu\mathrm{A/cm^2}$ (blue curve), but not when $I_{app} = 1\,\mu\mathrm{A/cm^2}$ (gray curve). The phase diagrams below show how the magnitude of current applied in epoch (b) determines whether or not the transition from V_{low} to V_{high} occurs.

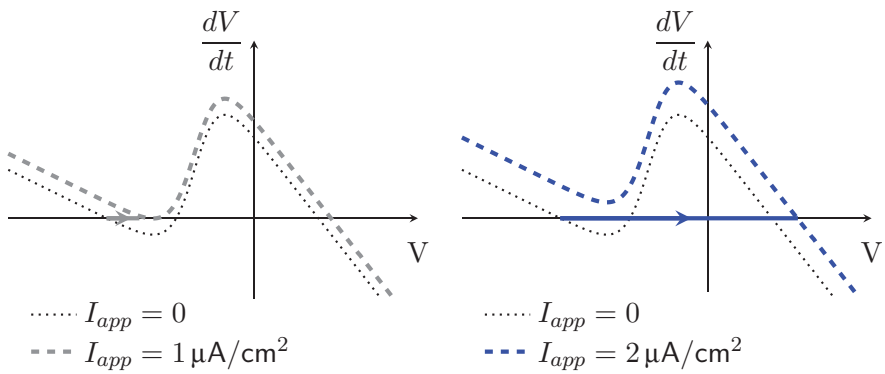

https://doi.org/10.1017/9780511793905.015 Published online by Cambridge University Press

11.4 Bifurcation Diagram for the Bistable $I_{\mathrm{Ca_V}} + I_L$ Membrane

Fig. 11.6 is a bifurcation diagram for the $I_{\mathrm{Ca_V}} + I_L$ membrane model that summarizes how the number and stability of steady state voltages depends on I_{app}. The range of applied currents that leads to bistability is $-6.4 < I_{app} < 1.0\,\mu\mathrm{A/cm^2}$. The critical values for applied current leading to fold bifurcations are labelled I^{**}_{app} and I^{*}_{app}.

The units and physical dimensions of Fig. 11.6 are mV (voltage, vertical axis) and μA/cm^2 (current/area, horizontal axis). Consequently, slope on this plot has physical dimensions of specific resistance (resistance/area) and units of kΩ/cm^2. This allows us to classify the stable steady states (solid blue curves) as belonging to the *low resistance branch* or *high resistance branch* (top and bottom, respectively).

The negatively sloped branch of unstable steady states in the bifurcation diagram of Fig. 11.6 may be described as the *negative resistance branch* (blue dashed curve). Its existence is related to the negatively sloped region of the membrane's current-voltage relation (Fig. 11.1), due to the negatively sloped region of the current-voltage relation for $I_{\mathrm{Ca_V}}$ that is the signature of a regenerative current (Fig. 10.3). Of course, the membrane conductances of the L-type channels ($I_{\mathrm{Ca_V}}$) and passive leak (I_L) are nonnegative quantities for any voltage. The *negative resistance* branch of steady states in the (I_{app}, V) bifurcation diagram (Fig. 11.6) and the *negative conductance* region of the current-voltage relation $I_{\mathrm{Ca_V}}$ (Fig. 10.3) and $I_{\mathrm{Na_V}}$ (Fig. 10.7) is a consequence of the voltage dependence of the conductance $g_{\mathrm{Ca_V}}$ and the electrochemical driving force $V - E_{\mathrm{Ca}}$ (see Discussion).

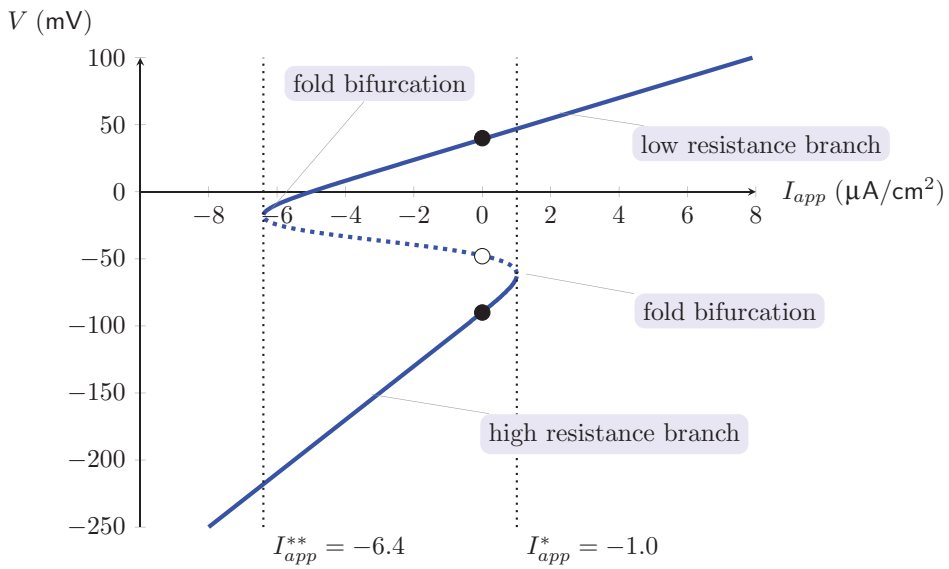

Figure 11.6 Bifurcation diagram for membrane model that includes $I_{\mathrm{Ca_V}}$ and I_L (Eq. 11.1). *Question*: Sketch qualitatively correct phase diagrams and phase lines for $I_{app} = I^{**}_{app}$ and I^{*}_{app}.

https://doi.org/10.1017/9780511793905.015 Published online by Cambridge University Press

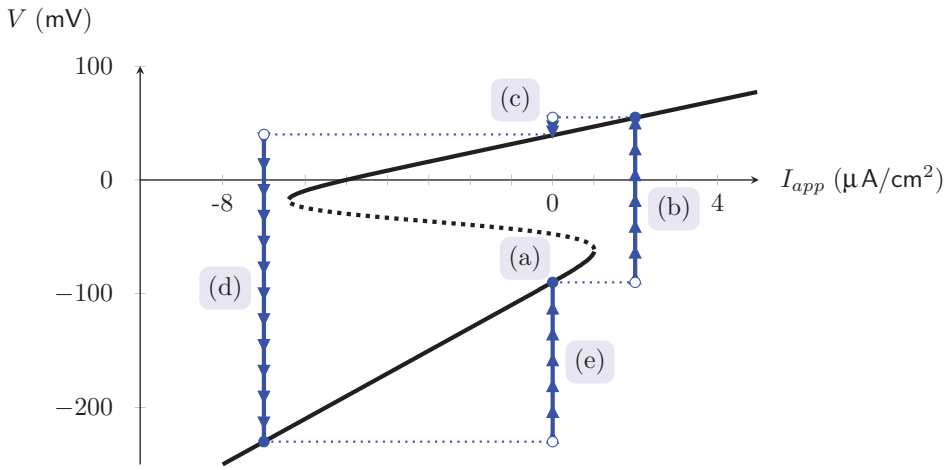

Figure 11.7 Overlaying trajectories (blue) on the bifurcation diagram (black) provides an interpretation of Fig. 11.4.

11.5 Overlaying Trajectories on the Bifurcation Diagram

Bifurcation diagrams provide useful summaries of the dynamics of membrane voltage. To illustrate, Fig. 11.7 plots a solution of the $I_{\mathrm{Ca_V}} + I_L$ membrane model (Fig. 11.4, blue curve) on top of the (I_{app},V) bifurcation diagram (black curve). The solution is a continuous function of voltage (vertical blue lines), but each change in applied current leads to a discontinuity in the (I_{app},V)-plane (horizontal dotted lines).

To understand the relationship between Figs. 11.4 and 11.7, find epoch (a) on both plots ($I_{app} = 0$ and $V = V_{low}$). The depolarizing step in applied current that occurs at $t = 100\,\mathrm{ms}$ causes the trajectory to shift rightward on the bifurcation diagram ($I_{app} = 0$ to $2\,\mu\mathrm{A/cm^2}$). During epoch (b) the solution moves upward toward the only attractor available when $I_{app} = 2\,\mu\mathrm{A/cm^2}$ (a depolarized steady state voltage). When the depolarizing current pulse ends, the trajectory instantaneously moves leftward to (c), then relaxes toward the steady state at V_{high}, and so on. Comparing Figs. 11.4 and 11.7 in this way, the response of the bistable membrane model to a sequence of applied current pulses is predictable.

11.6 Bistable Membrane Voltage Mediated by I_{Kir}

We showed that membrane potential bistability may occur in a neural membrane model (Eq. 11.1) that includes a passive leak (I_L) and an inward regenerative current ($I_{\mathrm{Ca_V}}$). In this section, we show how bistability may occur in membranes with an inward rectifying potassium current (I_{Kir}). Consider the membrane model

$$C\frac{dV}{dt} = I_{app} - \underbrace{\bar{g}_{\mathrm{Kir}} s_\infty(V)(V - E_{\mathrm{K}})}_{I_{\mathrm{Kir}}} - \underbrace{g_L(V - E_L)}_{I_L}, \tag{11.3}$$

https://doi.org/10.1017/9780511793905.015 Published online by Cambridge University Press

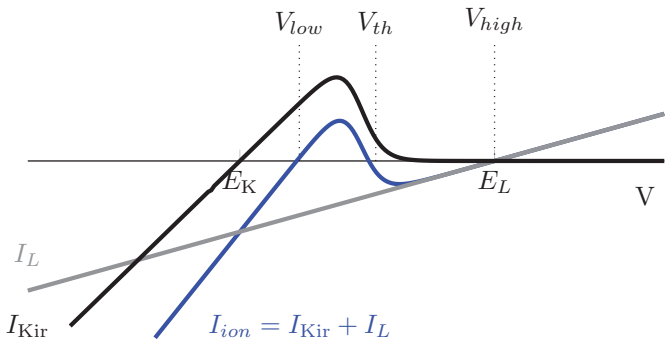

Figure 11.8 The sum of the ionic currents $I_{\rm Kir}$ and I_L may have three intersections with the horizontal axis $I_{ion} = I_{\rm Kir} + I_L = 0$. Because $V_{high} \approx E_L < 0$, this type of bistability is easily distinguished from bistability mediated by $I_{\rm Ca_V}$ and I_L (compare Fig. 11.1).

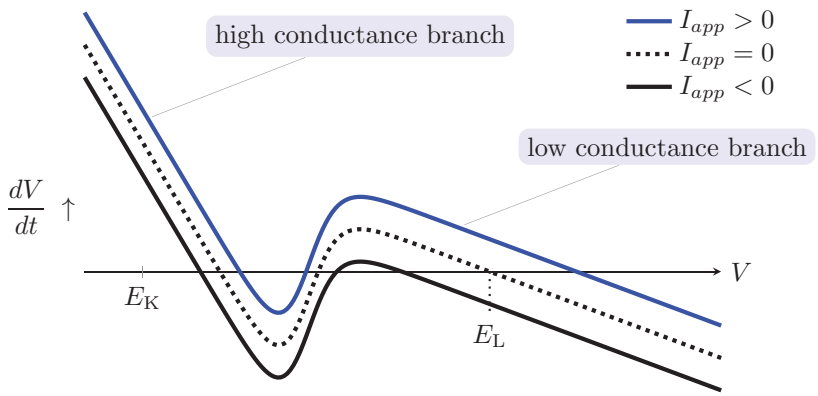

Figure 11.9 Phase diagram for the $I_{\rm Kir} + I_L$ membrane model (Fig. 11.8).

where $g_{\rm Kir}(V) = \bar{g}_{\rm Kir} s_\infty(V)$ is a decreasing sigmoidal function of voltage (as in Fig. 10.4). When the reversal potential for $I_{\rm Kir}$ is less than the reversal potential for the leakage current ($E_{\rm K} < E_L$),[1] the conductances $\bar{g}_{\rm Kir}$ and g_L can be chosen to yield a current-voltage relation for $I_{ion} = I_{\rm Kir} + I_L$ that reverses three times (Fig. 11.8). The slopes of the intersections with the horizontal axis indicate that the steady states at V_{low} and V_{high} are stable while V_{th} is unstable (Fig. 11.8). To see this, reverse the orientation of the vertical axis (flip up/down) and sketch arrows on the phase line (Fig. 11.9). Alternatively, one can reason that a steady state is stable if it occurs at a voltage for which the total membrane conductance is positive; for example, $dI_{ion}/dV\big|_{V=V_{low}} > 0$ and similarly for V_{high}. Conversely, a steady state is unstable if it occurs in a negative conductance region of the current-voltage relation where $dI_{ion}/dV < 0$.

There are qualitative similarities between the bistability mediated by $I_{\rm Kir}$ and $I_{\rm Ca_V}$ (compare Figs. 11.2 and 11.9). In both cases, the phase diagram has two negatively sloped branches and one positively sloped branch, separated by a local minimum and maximum. In both cases, the unstable steady state is a repellor that separates the basins of attraction of two stable steady states. Fig. 11.10 shows the salient quantitative

https://doi.org/10.1017/9780511793905.015 Published online by Cambridge University Press

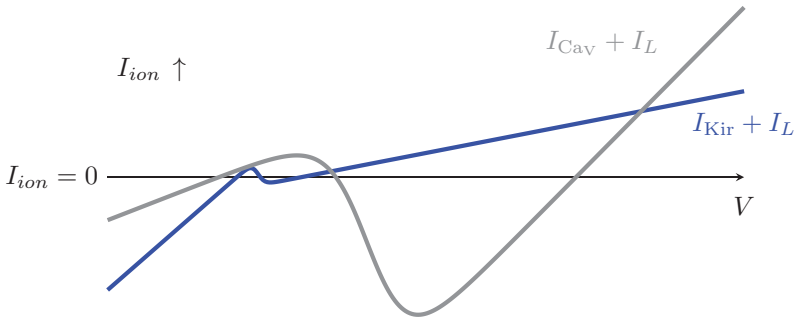

Figure 11.10 The I_{ion}-V relations for the $I_{\mathrm{Ca_V}} + I_L$ and $I_{\mathrm{Kir}} + I_L$ membrane models are qualitatively similar, but there are significant quantitative differences.

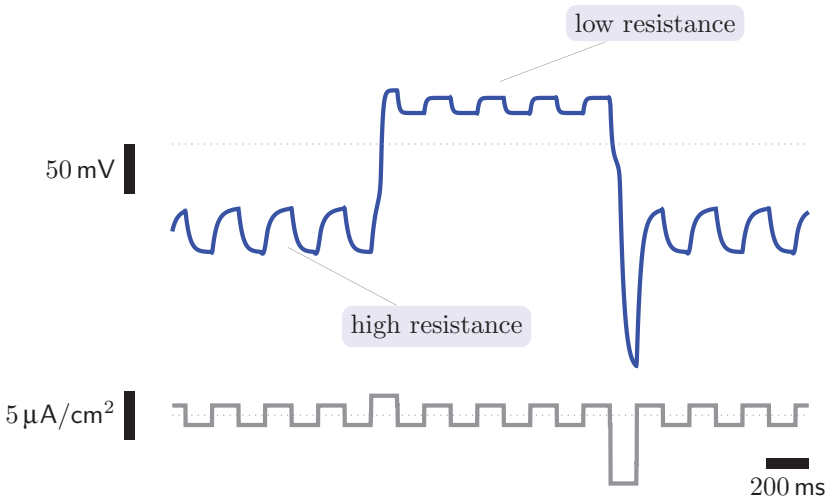

Figure 11.11 Bistability of the $I_{\mathrm{Ca_V}} + I_L$ membrane model (Eq. 11.1) observed in response to pulses of applied current (I_{app}).

differences. In the $I_{\mathrm{Ca_V}} + I_L$ bistable membrane, the depolarized steady state ($V_{high} \approx E_{\mathrm{Ca}}$) is the high conductance steady state (calcium channels open). In the $I_{\mathrm{Kir}} + I_L$ case, the depolarized steady state V_{high} is located near E_L (Kir channels closed), and the high conductance steady state is V_{low} (Kir channels open).

Fig. 11.1 shows a simulated current-clamp recording demonstrating that the depolarized steady state is high conductance (low resistance), as in the $I_{\mathrm{Ca_V}} + I_L$ membrane model.

11.7 Further Reading and Discussion

Spinal motor neurons of the brainstem and spinal cord exhibit $I_{\mathrm{Ca_V}} + I_L$ bistability and **plateau potentials**, defined to be a stable membrane potential that is more depolarized than the resting membrane potential (Hounsgaard et al., 1988; Perrier et al., 2002). α-motoneurons express action potential generating currents and innervate skeletal

https://doi.org/10.1017/9780511793905.015 Published online by Cambridge University Press

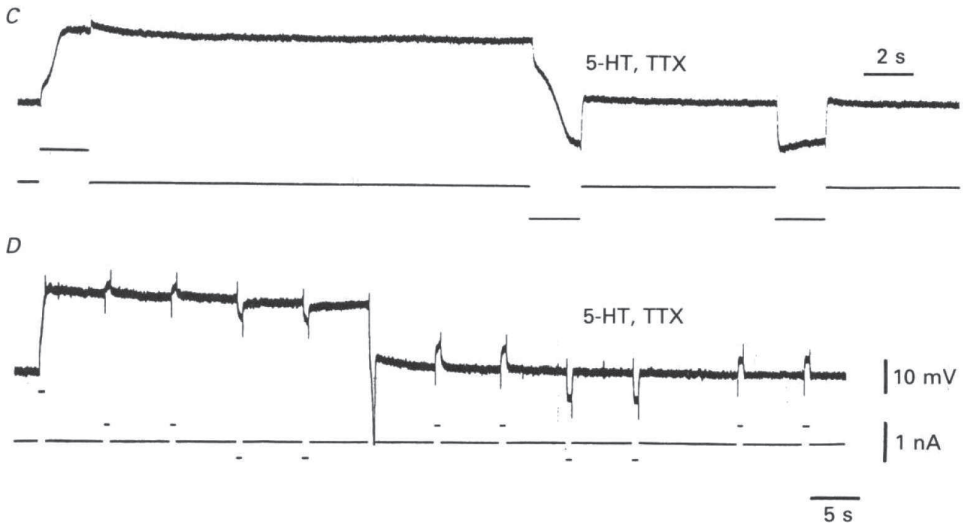

Figure 11.12 When action potentials of a spinal motoneuron are blocked by 1 μM tetrodotoxin (TTX), the neuronal membrane exhibits serotonin-induced plateau potentials (bistability). The membrane resistance is lower during the plateau than at rest. Reproduced with permission from Hounsgaard and Kiehn (1989), John Wiley and Sons.

muscle fibers; repetitive spiking of these neurons initiates muscle contraction. Plateau potentials are thought to support sustained action potential firing and to be useful in postural control (Kiehn and Eken, 1998).

Fig. 11.12 (top) shows an example in vitro intracellular recording from an α-motoneuron within a transverse section of the adult turtle spinal cord. When action potentials of a spinal motoneuron are blocked by 1 μM tetrodotoxin (TTX), the neuronal membrane exhibits plateau potentials (bistability) when stimulated by the neurotransmitter serotonin (10 μM). Fig. 11.12 (bottom) shows measurement of voltage change induced by depolarizing and hyperpolarizing current pulses of ±0.4 nA during the plateau (the depolarized steady state V_{high}) and at rest (the hyperpolarized steady state V_{low}). Consistent with Fig. 11.11, the membrane resistance was several fold lower during the plateau (V_{high} is the high conductance steady state).[2]

The voltage dynamics of bistable neurons in vivo is complicated by the activity of presynaptic neurons. The inevitable fluctuations in the magnitude of synaptic currents can cause the postsynaptic bistable neuron to spend irregular intervals of time in the low and high voltage states, a phenomenon known as *basin hopping*.

Fig. 11.13 shows an example of basin hopping in a striatal spiny neuron and a layer V cortical pyramidal cell, recorded simultaneously. $I_{\text{Kir}} + I_L$ bistability is thought to play a role in generating these plateau potentials (Wilson, 2008). In both cells, the depolarized steady state V_{high} is only a few millivolts from the action potential threshold and occasional spikes are observed when the neuron is in the depolarized plateau state. Observe that membrane potential fluctuations around the depolarized state are of higher amplitude than those around the hyperpolarized state. This is consistent with V_{low} being the high conductance steady state with open Kir channels (Fig. 11.9).

https://doi.org/10.1017/9780511793905.015 Published online by Cambridge University Press

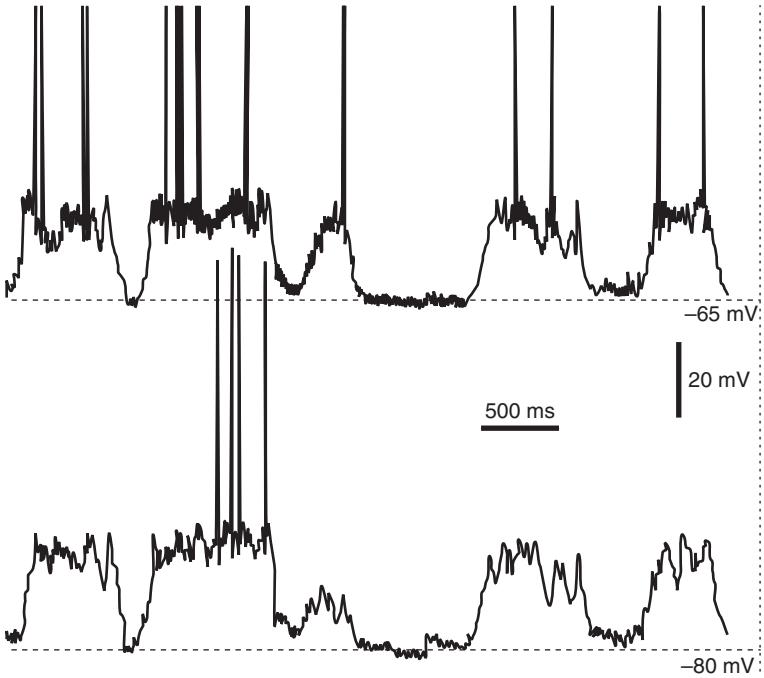

Figure 11.13 A simultaneously recorded layer V cortical pyramidal cell (top) and striatal spiny neuron (bottom) exhibiting plateau potentials (bistability) and basin hopping. Reproduced with permission from Charles Wilson (2008) Up and down states. Scholarpedia, 3(6):1410.

Membrane Conductance and Linearization

In the $I_{\mathrm{Ca_V}} + I_L$ membrane model (Fig. 11.3), the stability of the steady states at V_{low} and V_{high} is obvious from flow of these trajectories. Observe that for the initial voltages near a stable steady state, the solutions are approximately exponential. For each steady state, the total ionic current reverses by crossing the horizontal axis with a particular slope that has physical dimensions of conductance or conductance/area (Fig. 11.1). On the phase diagram (Fig. 11.2), slope has physical dimensions of (voltage/time)/voltage $=$ time^{-1}. The membrane model takes the form,

$$\frac{dV}{dt} = f(V) \tag{11.4}$$

and for each steady state V_{ss}, the function $f(V)$ crosses the horizontal axis with slope $f'(V_{ss})$. Observe that the Taylor series for $f(V)$ evaluated at each of these steady states is

$$f(V) = f(V_{ss}) + f'(V_{ss})\Delta V + f''(V_{ss})\frac{(\Delta V)^2}{2!} + f'''(V_{ss})\frac{(\Delta V)^3}{3!} + \cdots,$$

where $\Delta V = V - V_{ss}$. Remembering $f(V_{ss}) = 0$ (because V_{ss} is a steady state) and assuming that ΔV is small ($V \approx V_{ss}$), we may drop terms of order $(\Delta V)^2$ and higher to obtain

https://doi.org/10.1017/9780511793905.015 Published online by Cambridge University Press

$$f(V) \approx f'(V_{ss})\Delta V = f'(V_{ss})(V - V_{ss}) .$$

Substituting this approximate expression for $f(V)$ into Eq. 11.4, we obtain a linear ODE with solution that approximates solutions of the membrane model when $V \approx V_{ss}$,

$$\frac{dV}{dt} = f'(V_{ss})(V - V_{ss}) . \tag{11.5}$$

Furthermore, because V_{ss} was assumed to be stable, we know that $f'(V_{ss}) < 0$. If we write $\tau = 1/|f'(V_{ss})| > 0$ and substitute $f'(V_{ss}) = -1/\tau < 0$ in Eq. 11.5, we obtain

$$\frac{\text{voltage}}{\text{time}} \ominus \frac{dV}{dt} = -\frac{V - V_{ss}}{\tau} \ominus \frac{\text{voltage}}{\text{time}} ,$$

where $\tau \ominus \text{time}$ is an exponential time constant.

Problem 11.1 In the $I_{\text{Ca}_\text{V}} + I_L$ membrane model (Figs. 11.1–11.3), which stable steady state (V_{low} or V_{high}) has smaller time constant τ?

The Sign of dI_{ion}/dV Determines Stability

Normally we determine the stability of steady states using the phase diagram of an ODE model. However, the stability of the steady states of a membrane model may also be determined from the current-voltage relation. Recall that the phase diagram for the current balance equation takes the form $dV/dt = f(V)$ where

$$f(V) = \frac{1}{C}\left[I_{app} - I_{ion}(V)\right] .$$

Assuming constant I_{app}, differentiating $f(V)$ with respect to voltage gives

$$f'(V) = \frac{1}{C}\left[-I'_{ion}(V)\right] . \tag{11.6}$$

Steady states occur when $f(V_{ss}) = 0$; V_{ss} is stable when $f'(V_{ss}) < 0$ and unstable when $f'(V_{ss}) > 0$. Using Eq. 11.6 we can restate this fact in biophysical terms: steady states occur when $I_{app} = I_{ion}(V_{ss})$; V_{ss} will be stable if $I'_{ion}(V_{ss}) > 0$ and unstable if $I'_{ion}(V_{ss}) < 0$. (If this seems backwards, remember that in Eq. 11.6 $I'_{ion}(V)$ and $f'(V)$ have opposite sign.) For example, in the $I_{\text{Ca}_\text{V}} + I_L$ membrane model (Fig. 11.1), the steady states at V_{low} and V_{high} are stable, because $I'_{ion}(V_{low}) > 0$ and $I'_{ion}(V_{high}) > 0$. Conversely, the steady state at V_{th} is unstable ($I'_{ion}(V_{th}) < 0$). In fact, the slope of the current-voltage relation has a contribution from each current,

$$I'_{ion}(V) = I'_{\text{Ca}_\text{V}}(V) + I'_L(V) = I'_{\text{Ca}_\text{V}}(V) + g_L .$$

Because the contribution from the leakage current to this slope is positive, $I'_{\text{Ca}_\text{V}}(V_{ss}) > 0$ is a sufficient condition for stability in the $I_{\text{Ca}_\text{V}} + I_L$ membrane model. That is, beginning at V_{low} or V_{high}, a small change in voltage results in a restorative current (depolarization → outward, hyperpolarization → inward).

https://doi.org/10.1017/9780511793905.015 Published online by Cambridge University Press

Supplemental Problems

Problem 11.2 Explain why $I'_{\text{Kir}}(V_{ss}) > 0$ is a sufficient condition for stability in the $I_{\text{Kir}} + I_L$ membrane model (Figs. 11.8 and 11.9).

Problem 11.3 Answer the following questions for both the $I_{\text{Ca}_\text{V}} + I_L$ and $I_{\text{Kir}} + I_L$ bistable membrane models.

(a) The leakage current is inward when V is [greater / less] than [E_L / E_{Ca}].
(b) If I_{app} is increased the unstable steady state would move to a more [depolarized / hyperpolarized] voltage and eventually coalesce with the stable steady state associated with the [low / high] conductance branch of the current-voltage relation.
(c) This is an example of a [transcritical / fold / pitchfork] bifurcation.

Problem 11.4 Show that for brief, strong current pulses, the voltage will almost instantly reset to $V_* = V_{low} + \Delta V$ where $\Delta V = Q/C$ and charge $\ominus$ $Q = I_{app}\,\Delta t$ $\ominus$ current · time is the integrated current.

Solutions

Figure 11.1 V_θ is the voltage at which half of the calcium channels are open, that is, $m_\infty(V_\theta) = 1/2$ (Eqs. 10.1–10.3). V_θ can be located on the horizontal axis by plotting the current that would obtain if all channels were open, $\bar{I}_{\text{Ca}_\text{V}} = \bar{g}_{\text{Ca}_\text{V}}(V - E_{\text{Ca}})$. Then identify the voltage that leads to half this maximum voltage, that is, the V_θ that satisfies $\bar{g}_{\text{Ca}_\text{V}}(V_\theta - E_{\text{Ca}}) = \bar{I}_{\text{Ca}_\text{V}}/2$.

Figure 11.2 The exponential time constant is inversely proportional to the conductance of the membrane. Lower conductance corresponds to larger values of the membrane time constant $\tau = C/g$. So relaxation to V_{low} is slower than relaxation to V_{high} (see Fig. 11.3).

Figure 11.6 The phase diagrams and phase lines for $I_{app} = I^{**}_{app}$ and I^{*}_{app} are as follows.

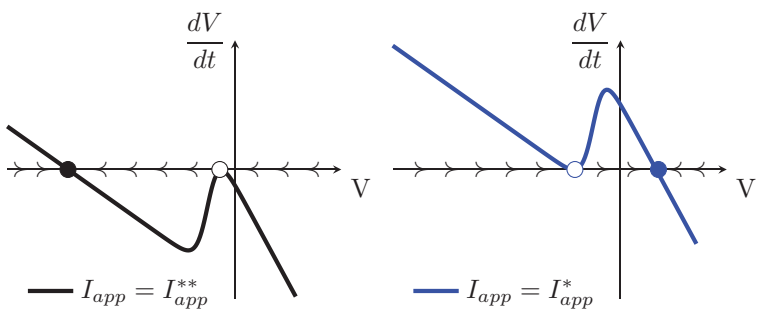

Problem 11.1 The high conductance steady state V_{high}.

https://doi.org/10.1017/9780511793905.015 Published online by Cambridge University Press

Problem 11.4 To see this, rewrite the current balance equation in the following way,

$$C\frac{dV}{dt} = I_{app} - I_{ion}(V) \;\Rightarrow\; \Delta V = \Delta t\,\frac{I_{app} - I_{ion}(V)}{C}\,.$$

Here we approximate $dV/dt \approx \Delta V/\Delta t$ where ΔV is the increment in voltage caused by the current pulse and Δt is the pulse duration. Substituting $I_{app} = Q/\Delta t$ where the charge Q is fixed, we find

$$\Delta V = \frac{Q}{C} - \Delta t\frac{I_{ion}(V)}{C}\,,$$

and taking the limit $\Delta t \to 0$ gives $\Delta V = Q/C$.

Notes

1. This could happen, e.g., if E_L is an effective Nernst equilibrium potential given by a weighted average of E_{Na} and E_{K}.
2. In Hounsgaard and Kiehn (1989) the membrane resistance was reported to be 2–4-fold lower during the plateau (4–10 mΩ) than at rest (14–18 MΩ).

https://doi.org/10.1017/9780511793905.015 Published online by Cambridge University Press